NEW DEVELOPMENT IN CENTRIFUGAL PUMPS FOR OPTIMUM CAVITATION PERFORMANCE

by

Moufak A. Zaher

Head of Research, Faculty of Applied Skills

Unitec Institute of Technology

Auckland, New Zealand

Moufak A. Zaher is Head of Research in the Faculty of Applied Skills, Unitec Institute of Technology, in Auckland, New Zealand. He is responsible for the applied research in both the building and transport departments. Dr. Zaher's previous experience includes lecturing on the subject of fluid mechanics, hydraulic research on pumps, turbines, radial and axial fans/blowers with special emphasis upon design, development, and computing. He has held the position of Technical Manager for several industrial projects.

Dr. Zaher received a B.S. degree (Mechanical Engineering, 1967) from Cairo University, and an M.S. degree (Mechanical Engineering, 1968) and Ph.D. degree (Engineering, 1972) from the Technical University of Lodz-Poland. He is an active member in both the Institute of Professional Engineers (New Zealand) and ASME. Dr. Zaher serves on Unitec's research advisory committees and is the author of several technical papers related to vortices, noise control, pumps, and fans.

ABSTRACT

During the past three decades, there have been notable advances in the design of pumps. In a number of projects, the designers of process plants had, during optimization of their layouts, established a requirement for pumps that outwits the standard ranges available from the majority of pump manufacturers. A considerable degree of technical expertise, backed by prototype development, is required if the benefits of high-speed operation are not to be offset by unreliability.

The flow within a centrifugal impeller is qualitatively unlike that in all other turbomachinery. The flow is very mixed, with strong influence of the viscous shear at the walls.

This paper describes how the rotational motion ahead of the impeller, created by partial bleeding from delivery side to the suction using suitable arrangements of nozzle units, has allowed the adoption of increased operating discharge pressures without embarrassingly high net positive suction head (NPSH) requirements.

INTRODUCTION

There are many places in process industries where low net positive suction head (NPSH) is required for pumping liquids that are at or near their boiling points. In general, anticavitation pumps using inducers can increase the suction specific speed of a high-speed pump by two to three times, thus giving a generous margin of safety in respect of permissible NPSH (Pearsall and Sobie, 1970; Sutton, 1967).

Various methods are open to increase NPSH available, but when substantial increase is required, usually the only practical solution is to install a separate low-speed booster pump upstream to the high-speed machine, as is current practice with boiler feedpumps (Sutton, 1967). An improvement in NPSH requirement can sometimes, and to a certain limit, be effected by changes in impeller geometry or the setup of fixed guide vanes.

The development of the proposed method of creating a rotary motion on the suction side using suitable nozzle arrangement has created an alternative solution, whereby reductions in NPSH requirements can be substantial. Rotary motion at suction can be used, at conventional speeds (i.e., 3600 rev/min and below), as a means of improving suction performance. One such application occurs in power stations where direct contact heaters are employed. These heaters require a heat extraction pump, and the use of rotary motion offers prospects of reducing the height of the heater above the pump. A reduction in height of the suction vessel above the pump is an attractive proposition whatever the application is.

In conventional pumps, as the NPSH is reduced, cavitation sets in, and eventually it becomes extensive enough to cause blockage of the blade passage with consequent loss of efficiency and head breakdown (Duncan, et al., 1971). The bleeding transferred to the suction side provides the low NPSH capability.

The rotary motion ahead of the impeller created by transferring part of the discharge energy back to the suction side using nozzles placed in a tangent position, suggests that the optimum values of capacity and pressure head can now be controlled from the suction side. Such bleeding transferred to the suction side provides the low NPSH capability, and generates sufficient head to prevent cavitation occurring inside the impeller, where the centrifugal impeller provides most of the head rise.

This paper reports on attempts made to measure the difference in the performance of pumps using partial bleeding from delivery side to suction, with those in conventional operation, similar to commercial types of moderate specific speed.

These data are presented and a discussion is given in which flow mechanisms are suggested to explain the observed results.

ADVANTAGES OF USING A BLEEDING SYSTEM WITH NOZZLE UNITS

To avoid the development of cavitation in the eye of a pump impeller, the absolute pressure at any point in the pump/impeller passages must be greater than the vapor pressure of the pumped fluid. This total pressure margin above the vapor pressure is termed the net positive suction head (NPSH). As fluid enters the impeller eye, static head is converted into velocity head due to the increase in absolute velocity. A loss in total head results from interaction between the fluid and the leading edges of the impeller vanes.

A supercavitating pump is designed to achieve bubble collapse away from the blades. However, while the blade surface may escape damage, the blade tip and surrounding casing may not. The main advantage claimed for supercavitating devices such as inducers is difficult to assess.

The main concern with using inducers is cavitation erosion and narrow operating range. Since it is a cavitating device, it must be looked upon as a consumable item. Material with good cavitation erosion resistance is clearly required for the inducer and its casing (Kratzer, 1975).

Inducers have also been known to produce instabilities and should always be checked for permissible operating range. High solidity is a prerequisite of low vane loading, therefore, an inducer will tend to be less efficient than a conventional axial flow impeller of the same specific speed because of additional vane friction.

In view of all the foregoing, a certain amount of caution in their application certainly seems warranted.

The development of the suggested bleeding system, which operates on the transfer of part of the discharge energy back to the suction side to form a rotating motion before the impeller by using suitable nozzle units (Figure 1), has created an alternative solution. It is destined to take over the role of inducers, or similar devices, operating with the same suction specific speed, as cavitation erosion and vibration are almost unaccounted for in the new system. With the new system, operation under partial cavitating conditions is possible while still supplying sufficient head to the impeller. With flow angle at the inlet of the impeller now made greater, it is easier to work on new impeller designs (Reddy and Pickford, 1979). Fewer numbers of vanes are now possible with the result of attaining a higher pump efficiency.

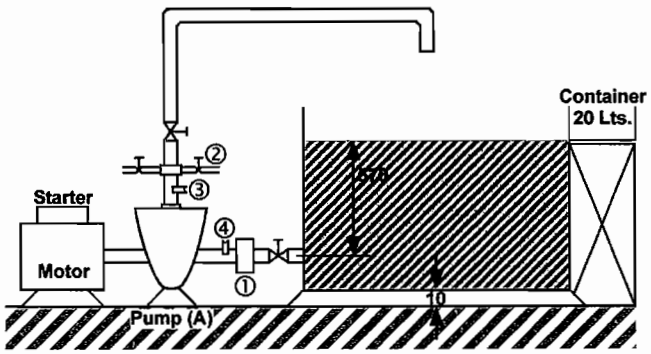

1. Nozzle Unit
2. Bleed
3. Discharge Pressure Tap
4. Suction Pressure Tap

Figure 1. Test Facility for Pump A.

DIMENSIONLESS NUMBERS

Several dimensionless numbers were examined to assist in explaining the flow mechanism of the new pump arrangement. Among these dimensionless numbers are the Rossby and Reynolds numbers.

Rossby Number

For a given flow and speed, the diameter (d_n) was found to depend on the Rossby number (Ro = Vr/ωRn) at the entrance to the impeller, and hub/tip ratio, λ. This number is expressed as the ratio of the acceleration due to curvature and that due to Coriolis forces. For low NPSH, the Rossby number should be as small as possible. It was found that *Ro* for the new pump arrangement is about seven percent less in value than that for the conventional pump, ranging from 0.7 at the impeller entrance to 0.25 at exit.

Reynolds Number

Although the Reynolds number (*Re*) was found to be in the range of $Re = V D_s/\nu = 10^5$ at the inlet to the impeller, in general it should be realized that this number for the flow through the nozzle jet does not possess the properties of the Reynolds number associated with the straight pipe flow, and, therefore, cannot serve as an actual guide including criterion of the performance of the pump.

Neither the Rossby nor the Reynolds numbers or any of the other conventional dimensionless numbers served as a good guide to explain the performance of the new pump. A proposed dimensionless number is introduced for this purpose named the "Bleeding Number."

Bleeding Number

The mixing expected in the impeller will increase the loss, both due to increased frictional loss and due to the mixing itself. However, the highly backswept design of blades and uniform flow will decrease nozzle loss. With this in mind, it is clear that development of conventional pump designs requires modification work.

However, in examining our case, and in order to explain the basic mechanism of the vortex created ahead of a centrifugal impeller for the new pump, we use a dimensionless group called the Bleeding Number, $B_N = NACd/Qw$ (refer to APPENDIX A for the mathematical derivation). This number is essentially the ratio of the quantity of flow from the nozzles to the quantity of flow going to the impeller. In a rotor, a particle of fluid, stationary in the relative frame, can withstand a significant radial pressure gradient without relative acceleration. When there are pressure changes associated with a forced vortex, motions of this sort are subtracted from the static pressure and what is left is the reduced static pressure. In the absence of friction, a stationary particle on the rotor will accelerate due to the gradient of reduced static pressure. Once it has gained a relative velocity, acceleration will come into force. Gradients of reduced static pressure are thus what drives the formation of vortex flow. These gradients are introduced by either curvature of streamlines in the relative frame or by acceleration. Streamline curvature in a centrifugal impeller is introduced by the effect of flow acceleration from nozzles, the meridional bend from axial to radial, and the curvature of the blades themselves. The forces associated with acceleration are introduced into the flow by the blade loading. In the new centrifugal pump, both the nozzle effect and the meridional bend influence the early part of the flow. The gradients of the total pressure may have one of the two origins. These are either convected into the rotor or induced by shear in the boundary layers of the rotor.

Hypothetically, the comparison between the function of guide vanes and the proposed vortex motion created on the suction side by the bleeding system indicate that: while the vanes merely guide the fluid to a certain direction with an increase in its velocity, the proposed bleeding system, on the other hand, is a supplier of pressure energy and also imparts, through a set of nozzle units, a tangential acceleration. The function of the proposed bleeding system is very similar to that of an impeller.

DESIGN AND PERFORMANCE CHARACTERISTICS

The development of bleeding pumps has been undertaken at the author's company for a number of months, including the different arrangements of nozzle units combined with the centrifugal pump machine. In designing the model and prototype pump of this type, a number of factors had to be taken into account. This could be obtained by changing the inlet size of the pump to meet the need for various flows, and changing the centrifugal impeller diameter to give the heads required. Further extension of the range is provided by a choice of pump speeds.

Ideally it would be convenient to add the bleeding system to a standard centrifugal pump. In plant usage, the ability of the pump to run satisfactorily at off-design conditions is necessary, both at higher NPSH and lower flows than the design conditions. Neither of these appeared to impose any problems, although cavitation or erosion damage would be unlikely to be worse than in a conventional pump.

The first item in the design process was to decide on the optimum diameter (d_n) and the position of the nozzle unit on the suction side. The nozzles had to be specially designed to avoid possible flow separation and minimize other friction losses. This would probably mean avoiding the sharp edges and steep tapering ideally required on a nozzle unit.

Mechanically, impeller rotor balance was not a problem, and bearings and seals followed standard practice. It was necessary that the pump could be withdrawn completely without disturbing the pipe work. For this reason, spacers had to be inserted between the pump and the nozzle unit.

The performance of pumps is of increasing importance in "energy consciousness." The shape of the pump characteristic and its suction performance (cavitation) is also of extreme importance.

In order to improve these designs, better understanding of and ability to predict the flows encountered in the pump are required. The first step was to investigate the internal flow. The second, armed with the insight gained, was to predict the performance of new designs.

Accordingly, an essential part of the project was to investigate typical industrial pumps. The pumps selected represented three duties in which the operators can have cavitation problems with conventional pumps. In such an evaluation, it was important that the prototype site should not be wholly dependent upon this new pump and, for this reason, the new pump was put in parallel with the existing pumps, which then remained on standby. The duties are shown in Table 1.

Table 1. Pump Duties.

	A	B	C
Product	Water	Water	Water
Pumping fluid temp.	Ambient	Ambient	Ambient
Specific gravity	1.00	1.00	1.00
Vapour press.	2.55x102 kg/m2	2.55x102 kg/m2	2.55x102 kg/m2
	0.36 Psi Abs.	0.36 Psi Abs.	0.36 Psi Abs.
Capacity	0.8 L/s	20 L/s	5 L/s
Differential head	2 m	4.5 m	3.5 m
NPSHA	0.5 m	1.5 m	0.75 m

TEST FACILITY AND INSTRUMENTATION

Pump A

The test facility used in this investigation is a closed loop hydraulic circuit. A sketch is shown in Figure 1. Its components are described in APPENDIX B.

Nozzle Units Used with Pump A

Nozzles fixed on the suction side of each test are made of aluminum so that the effect of corrosion and abrasion on the change of friction losses would be negligible. The nozzles were machined at workshops outside the author's company, and the finishing touches with fittings were partly made at onsite workshops, and at the test stand. Figure 2 shows the nozzle units, 2N × 3mm d_B, and 2N × 6 mm d_B, used with Pump A. Table 2 gives the dimensions of the used nozzles.

Table 2. Dimensions of Nozzle Units Used with Pump A.

	Nozzles (number)	Bleed pipe diam. to nozzle (d_B) mm	Nozzle head diam. (d_n) mm	Length of taper (L_n) mm
a	2/4	3	1.5	6
b	2/4/two series	6	3	12
c	2/4/two series	12	6	24
d	4	12	3	24
e	2/4/two series	19	9.5	38
f	2/4	19	4	38

The driving head, H_d, for the bleed part is measured from the test facility. The capacity, Q_0, enters the pump suction with a head, H_0, which is also measured on the pump. The capacity entering the impeller equals the sum of that due to the suction, Q_0, and that due to the bleed, Q_d:

$$Q_W = Q_0 + Q_d \quad (1)$$

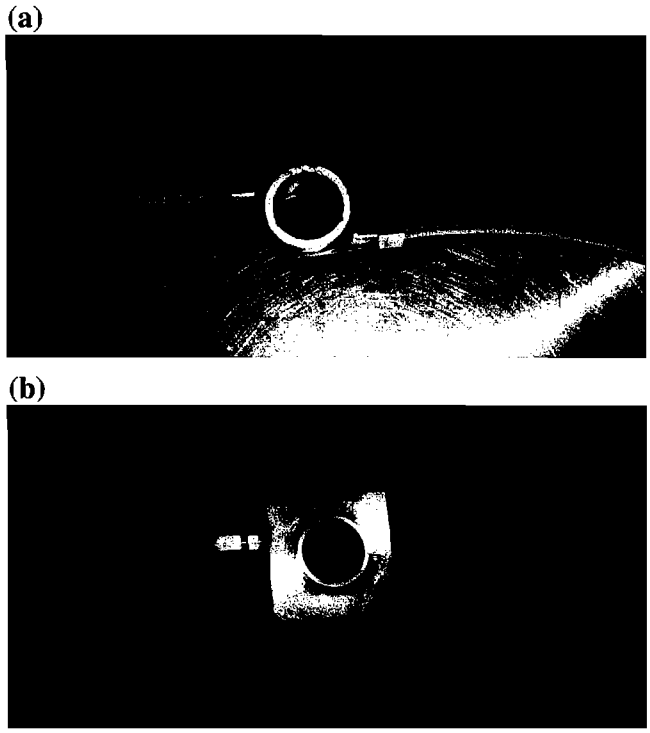

Figure 2. Nozzle Units (2N-3, 2N-6).

The flow, Q_d, through the nozzle is normally calculated by assuming a maximum value for the bleed that causes the rotation ahead of the impeller on the suction side. The discharge flow from the nozzle (Q_d) is,

$$Q_d = N\,A\,C_d \quad (2)$$

where:
N represents the number of nozzles
A is the cross sectional area of the nozzle
C_d is the fluid absolute velocity at nozzle exit

Reference is also made to APPENDIX A.

Calibration Test for Pump A

These tests were performed to study the behavior of the pump performance using the bleeding system from the delivery side to the suction side. Tests were performed in steady, nonpulsating conditions, and almost constant temperature (records showed a negligible rise in temperature between the pump suction and pump delivery, in average not exceeding 0.5°C. One effect could be the hot air discharged from the pump electric motor and directed toward the pump impeller). The motor was operating at the service factor horsepower, i.e., operating at safe temperatures.

Each of the following tests involved three positionings of the pump (Figure 3):

- When the level of the water tank is 105 mm above the suction valve (Figure 3(a)).
- When the level of the water tank is 557 mm above the suction valve (Figure 3(b)).
- With a suction lift of 875 mm from the center of the suction pipe (Figure 3(c)).

The photos in Figure 4 (i, ii, iii) show the corresponding setup of different nozzle units ahead of the pump on the suction side. Four groups of tests were performed.

In the first group of tests, two configurations of nozzle units (all type "a," Figure 2(a)) were used. These were:

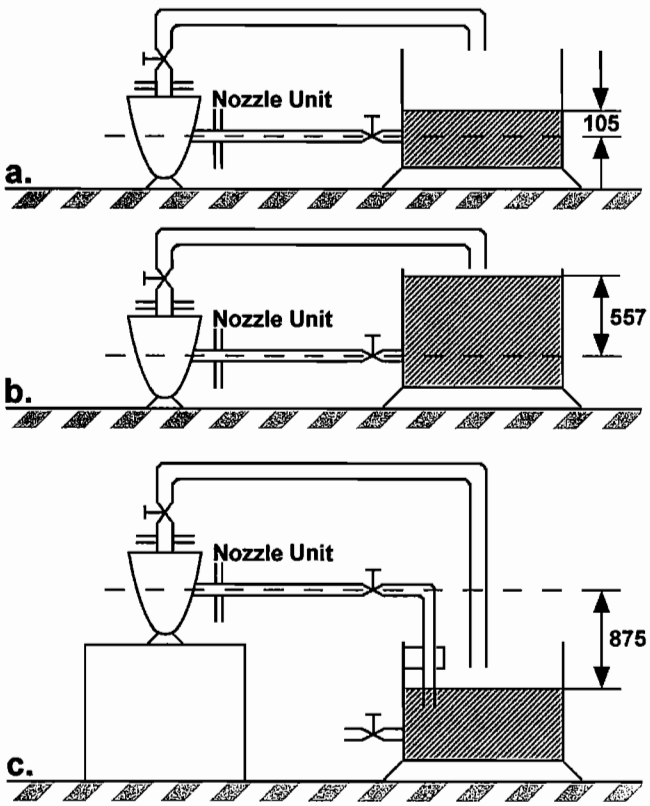

Figure 3. The Three Different Testing Levels for Pump A.

- Two nozzles × 3 mm d_B
- Four nozzles × 3 mm d_B

Each of these units was tested to find the optimum resolutions when working on the following parameters:

- Delivery valve: Fully open (FOV), ½ open (½ OV), ¼ open (¼ OV), and fully shut (FSV)
- Bleeding valves: Fully closed, fully open, ½ open, and ¼ open
- Nozzle position from impeller inlet: Five different positions, i.e., 68 mm, 85 mm, 100 mm, 125 mm, and 200 mm
- Direction of rotation of swirling flow from the nozzle: To be set once with the same direction of rotation as that of the impeller, and another against the direction of rotation of the impeller

In the second group of tests, four configurations of nozzle units (all type "b," Figure 2(b)) were used. These were:

- Two nozzles × 6 mm d_B
- Four nozzles × 6 mm d_B
- 2 × 2 nozzles in series at three different mutual distances (15, 40, and 60 mm apart) × 6 mm d_B
- 2 × 4 nozzles in series at three different mutual distances (15, 40, and 60 mm apart) × 6 mm d_B

Each of these units was tested in the following positions and combinations:

- Delivery valve: Fully open, ½ open, ¼ open, and fully shut
- Bleeding valves: Fully shut, fully open, ½ open, and ¼ open
- Nozzle position from impeller inlet: 65 mm, 85 mm, and 100 mm
- Direction of rotation of flow from the nozzle: With the same direction of rotation as that of the impeller

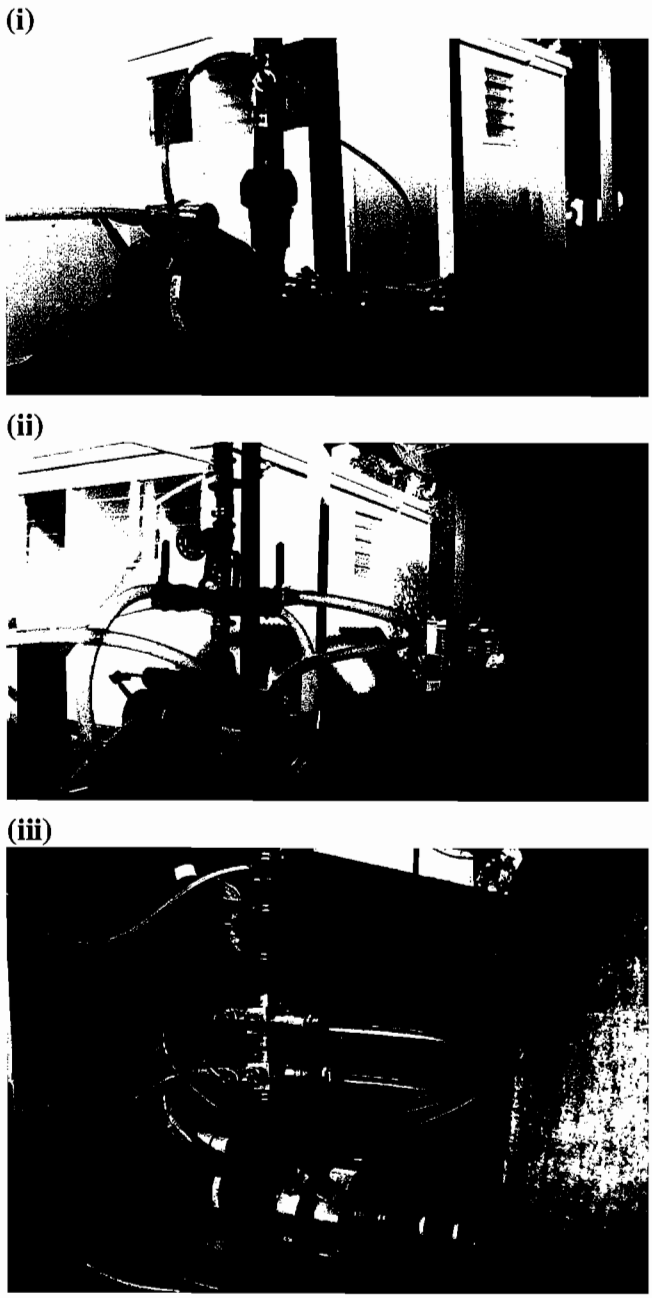

Figure 4. Photos of Pump A at Different Levels.

In the third group of tests, five configurations of nozzle units were tested. These were:

- Two nozzles × 12 mm d_B
- Four nozzles × 12 mm d_B
- 2 × 2 nozzles in series at one mutual distance (40 mm apart) × 12 mm d_B
- 2 × 4 nozzles in series at two mutual distances (40 and 80 mm apart) × 12 mm d_B
- Four nozzles × 12 mm d_B (3 d_n)

Each of these units was tested in the following positions and combinations:

- Delivery valve: Fully open, ½ open, ¼ open, and fully shut
- Bleeding valves: Fully shut, fully open, ½ open, and ¼ open

- Nozzle position from the impeller: 65 mm
- Direction of rotation of flow from the nozzle: With the same direction of rotation as that of the impeller

In the fourth group of tests, six configurations of nozzle units were tested. These were:

- Two nozzles × 19 mm d_B
- Four nozzles × 19 mm d_B
- 2 × 2 nozzles in series at three mutual distances (40 and 80 mm apart) × 19 mm d_B
- 2 × 4 nozzles in series at three mutual distances (40 and 80 mm apart) × 19 mm d_B
- Two nozzles × 19 mm d_B (4 d_n)
- Four nozzles × 19 mm d_B (4 d_n)

Each of these units was tested in the following positions and combinations:

- Delivery valve: Fully open, ½ open, ¼ open, and fully shut
- Bleeding valves: Fully shut, fully open, ½ open, and ¼ open
- Nozzle position from the impeller: 65 mm
- Direction of rotation of flow from the nozzle: With the same direction of rotation as that of the impeller

Test Observations for Pump A

The following observations were derived from the calibration test for Pump A:

- *Direction of rotation of the swirling flow from nozzle unit*—The analysis of data for both positive (same as the direction of impeller motion) and negative (against the direction of the impeller motion) rotations of flow from the nozzle units demonstrated an appreciable pressure detection when compared to conventional pumping. On the other hand, the head-discharge characteristics were found to be higher in the case of positive rotation as compared to negative rotation, affirming more stable conditions, and reduced separation at entrance of the impeller.

- *Location of nozzle units ahead of the impeller*—Test results showed that better values for ΔH are reached with nozzle unit approaching closer to the impeller. This can be explained by the fact that, as the particles of rotating fluid get closer to the impeller, the absolute velocity increases due to the influence of centrifugal forces caused by rotating motion on the nozzle side. Consequently, a higher change in pressure on the suction side is generated.

These results are in agreement with what was indicated earlier, that the function of the flow from the nozzle unit placed before the impeller is very similar to that of the conventional impeller. It is not right to compare the proposed arrangement of the bleeding system (with suitable nozzle design) to the function of guide vanes or the effect of particle prerotation (whirl) due to the influence of impeller blading.

- *Shape and design dimensions for the nozzle unit*—The role of the nozzle has been made easier by giving it the best shape to achieve the highest possible ΔH. A single four nozzle unit gave the best increase in ΔH. Using this shape, the mixing process ensured a reasonable uniform flow to the impeller. This was in contrast to other shapes in which substantial losses occurred inside the nozzle channels, giving lower values of ΔH. Figure 5 shows the optimum dimensions recommended for the nozzle shape.

Pump B

A closed loop hydraulic circuit is used in this investigation (Figure 6). Its components are described in APPENDIX C.

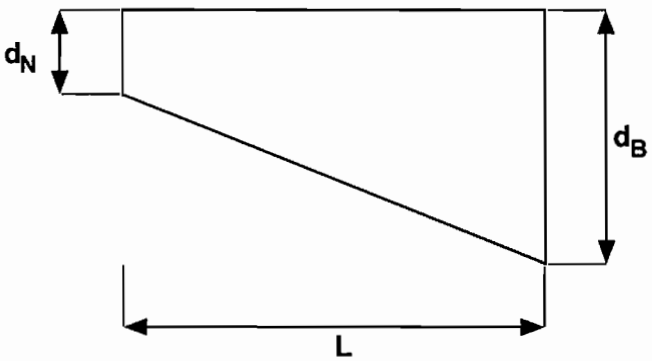

Figure 5. The Optimum Geometrical Dimensions of Nozzle Unit. (d_B: d_n = 2:1, d_B: L = 1:2)

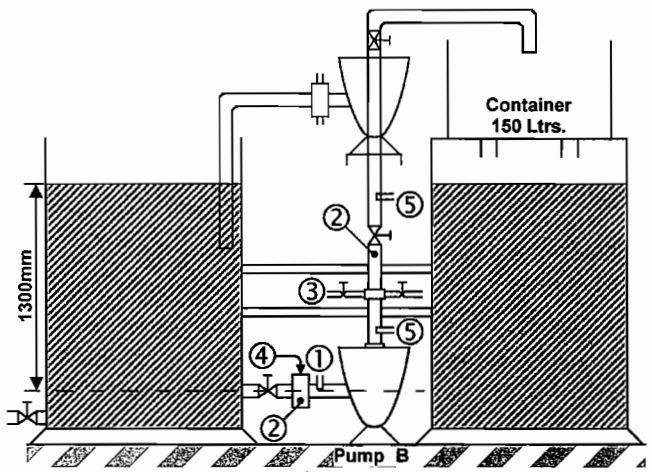

1. To pressure manometer
2. Temperature detector
3. Bleeding control system
4. Nozzle unit
5. Discharge pressure tap (gauge)

Figure 6. Test Facility for Pump B.

Nozzle Unit for Pump B

The nozzle unit for Pump B is shown in Figure 7 (four nozzles, d_B = 40 mm, d_n = 20 mm, and L = 80 mm). The flow through the nozzle unit, Q_d, was calculated in a similar way as that for Pump A (refer to Equation (1).

Calibration Test for Pump B

Tests were performed to study the behavior of the pump performance using a bleeding system from the delivery side to the suction side. Tests were performed in steady, nonpulsating conditions, and almost constant temperature. Records showed a negligible rise of temperature between the pump suction and pump delivery, in average not exceeding 0.5°C. The motor was operating at the service factor horsepower. Figure 6 shows the nozzle unit ahead of the pump on the suction side.

The tests involved three positionings of the pump:

- When the level of the water tank is 500 mm above the suction valve
- When the level of the water tank is 1300 mm above the suction valve
- With a suction lift of 1500 mm from the center of the suction pipe

The dimensions of the nozzle unit are (Figure 7):

- Four nozzles × 40 mm d_B × 20 mm d_N × 80 mm L

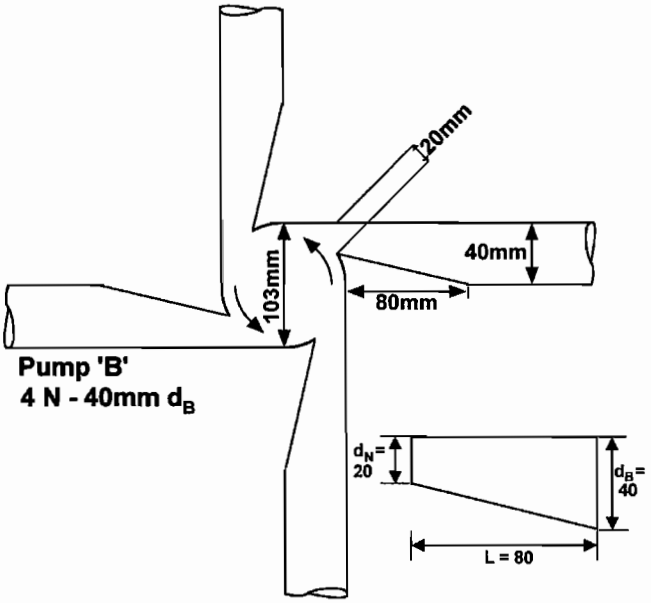

Figure 7. Nozzle Unit (4N-40) for Pump B.

The nozzle unit was tested for the following parameters:

- Delivery valve: Fully open, ½ open, ¼ open, and fully shut
- Bleeding valves: Fully closed, fully open, ½ open, and ¼ open
- Nozzle position from the pump inlet flange is 130 mm, 490 mm from the suction tank, and 390 mm from the suction valve
- Direction of rotation of the swirling flow from the nozzle: The same direction of rotation as that of the impeller

Pump C

Test Facilities for Pump C

The same test facilities used for Pump B were also used for Pump C, with necessary modifications described in APPENDIX D (Figure 8):

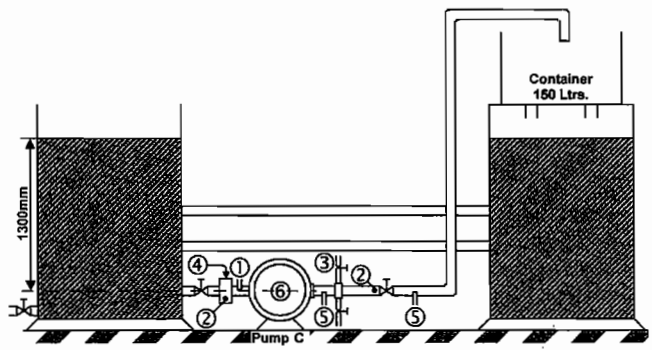

1. To pressure manometer
2. Temperature detector
3. Bleeding control system
4. Nozzle unit
5. Discharge pressure tap (gauge)
6. Side inlet – side outlet pump

Figure 8. Test Facility for Pump C.

The Nozzle Unit for Pump C

The nozzle unit for Pump C is shown in Figure 9 (four nozzles, d_B = 25 mm, d_n = 12.5 mm, and L = 50 mm). The nozzle unit is placed at a distance of 230 mm from pump centerline. The flow through the nozzle unit, Q_d, was calculated in a similar way as that for Pumps A and B (refer to Equation (1).

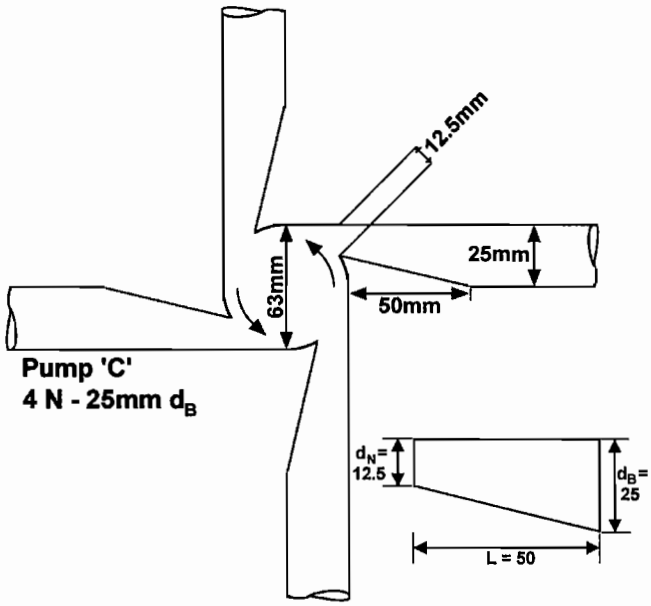

Figure 9. Nozzle Unit (4N-25) for Pump C.

Calibration Test for Pump C

The tests involved two pump positions:

- When the level of the water tank is 500 mm above the suction valve
- When the level of the water tank is 1300 mm above the suction valve

The nozzle unit was tested for the following parameters:

- Delivery valve: Fully open, ½ open, ¼ open, and fully shut
- Bleeding valves: Fully closed, fully open, ½ open, and ¼ open
- Nozzle position from impeller centerline: 230 mm and 12 mm from pump suction flange
- Direction of rotation of flow from the nozzle: The same direction of rotation as that of the impeller

TEST RESULTS AND PERFORMANCE CHARACTERISTICS

The three pumps were tested at the author's company. Details of these pumps are shown in Table 3.

Table 3. Pump Details.

Pump	A	B	C
Speed rpm	1400	1390	1450
Flow L/S (gpm)	0.8 (12.7)	20 (317)	5 (79.3)
Head m (ft)	2 (6.6)	4.5 (14.8)	3.5 (11.5)
Inlet diameter mm	20	60	60

Figure 10 shows incipient cavitation before the nozzle unit (4 N × 6/12 mm d_B) at suction side, and elimination of cavitation after the nozzle unit for Pump A.

Figures 11, 12, and 13 show the optimum bleeding required at three different positions (875 mm suction lift, 557/105 mm suction head) for Pump A, using different shapes of nozzle units. It was found that the optimum bleeding occurred in the range between B_N = 0.03 to 0.04. It was also noticed that the flow tends to be unstable as the Bleeding Number values approach B_N = 1.

APPENDIX E lists the results for the total range of nozzle units used for Pumps A, B, and C at different levels. Figures 14, 15, 16, 17, 18, 19, 20, and 21 and APPENDIX W show the complete characteristic curves including the head flow, pump efficiency

Figure 10. Photos Showing Effect of Nozzle Units on Incipient Cavitation (2N-6, 4N-12).

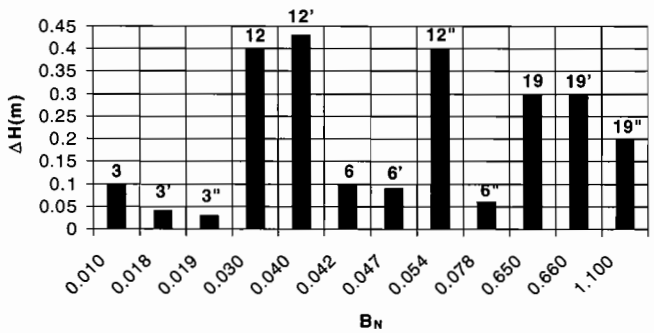

Figure 11. Optimum Bleeding Curve—Suction Lift (875 mm) FOV = 1/2 OV to 1/4 OV.

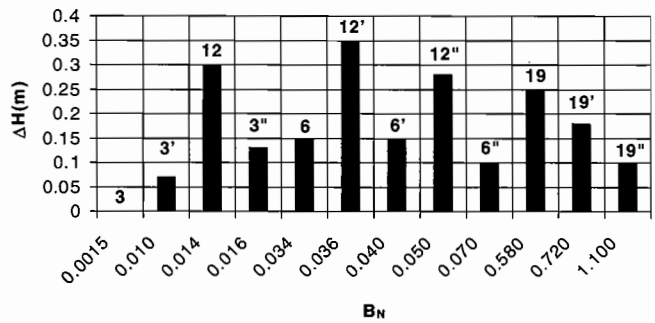

Figure 12. Optimum Bleeding Curve—Suction Head (557 mm) FOV = 1/2 OV to 1/4 OV.

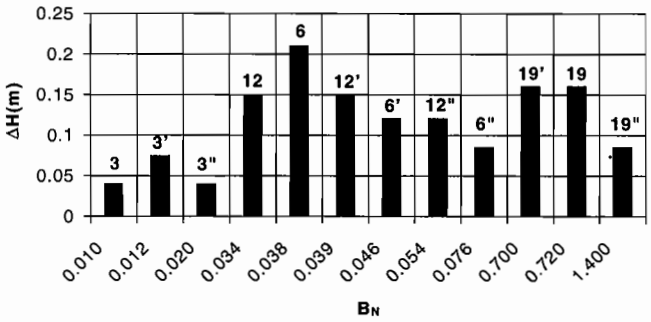

Notation:

FOV =	Fully open discharge valve
½OV' =	Half open discharge valve
¼OV" =	Quarter open discharge valve
B_N =	Bleeding number (dimensionless)
ΔH =	Difference between total head for the new arrangement minus the total head for conventional pump

Figure 13. Optimum Bleeding Curve—Suction Head (105 mm)— FOV = 1/2 OV to 1/4 OV.

(defined as Q_0 H × SG)/Bhp), and break-horsepower at the pump shaft for the conventional and new arrangement of pumps: A (using the best nozzle arrangement of: 4 N × 12 mm d_B), B (using nozzle unit: 4 N × 40 mm d_B), and C (using nozzle unit: 4 N × 25 mm d_B). The efficiency given is the overall pump efficiency including the motor, which means a peak efficiency of 80 percent for Pump A (Table E-1), 86 percent for Pump B (Table E-4), and 82 percent for Pump C (Table E-5), as compared with conventional pumps of 70 percent, 70 percent, and 72 percent, respectively.

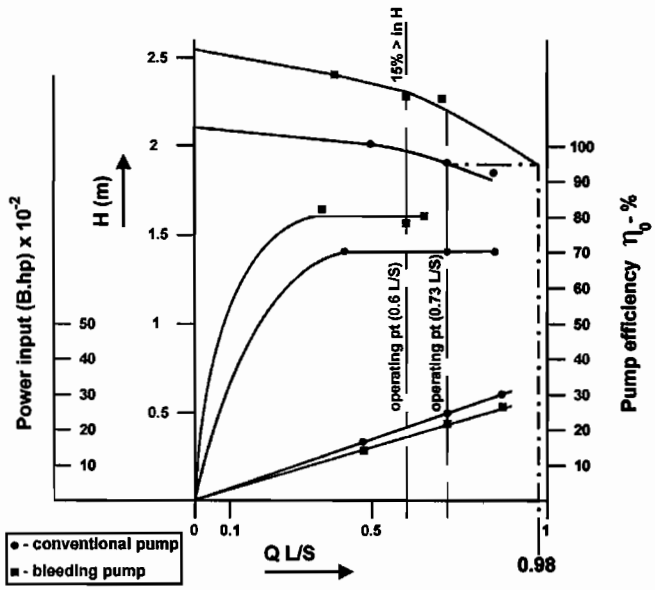

Figure 14. Characteristic Curve for Pump A—Suction Lift, 875 mm.

Figures 22, 23, 24, and 25 show the cavitation characteristics with optimum bleeding using the best nozzle arrangement (4 N × 12 mm d_B and 4 N × 40 mm d_B) for Pumps A and B. They represent the values of $NPSH_A$ (defined as: $NPSH_A$ = atmospheric pressure + static head + pressure head—vapor pressure of the fluid—loss in the piping, valves, and fittings) resulting from the use of a specific nozzle, i.e., increase of $NPSH_A$ compared to a base point, A_{Conv}. The curve also shows points corresponding to other configurations of nozzle units.

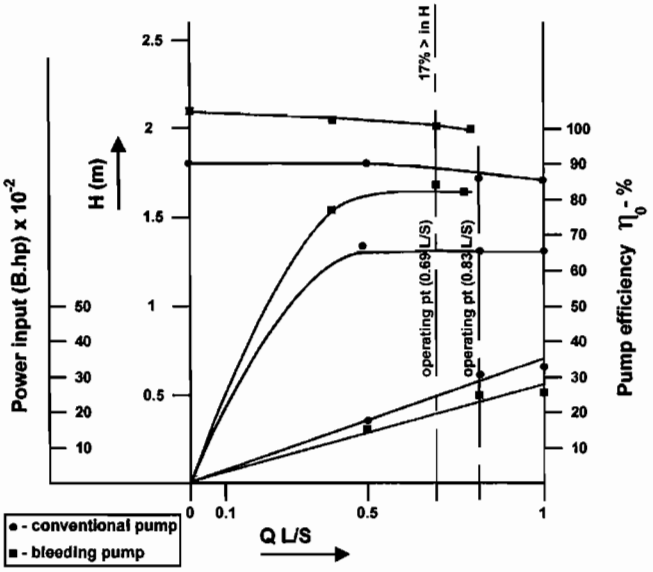

Figure 15. Characteristic Curve for Pump A—Suction Head, 556 mm.

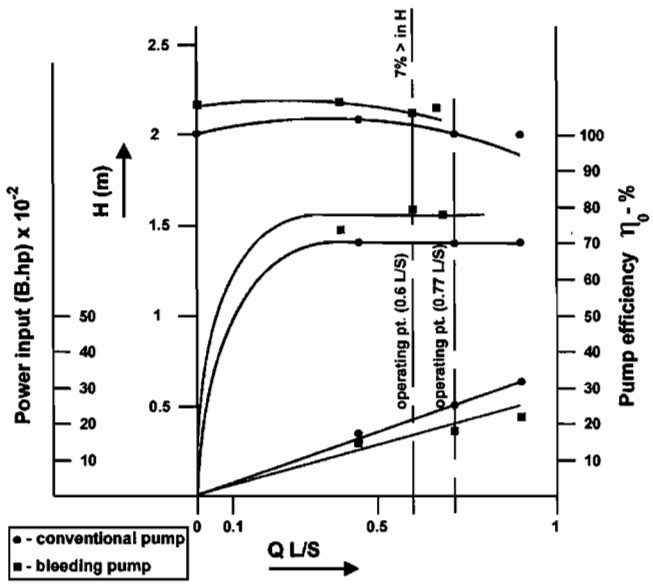

Figure 16. Characteristic Curve for Pump A—Suction Head, 105 mm.

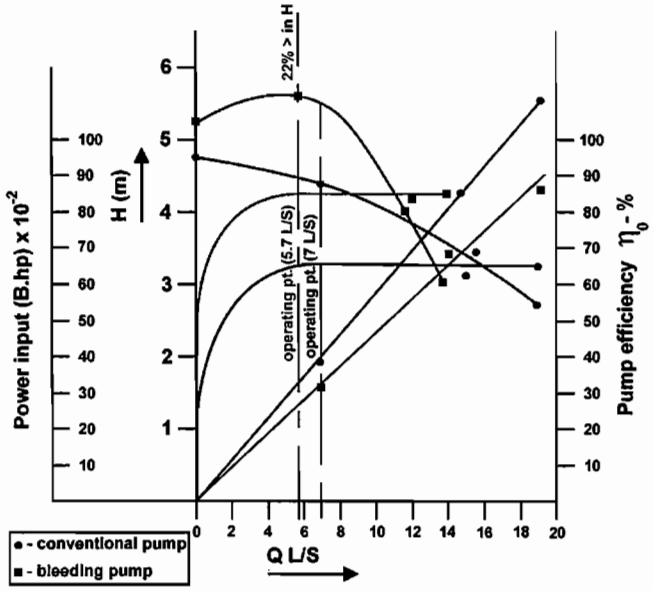

Figure 17. Characteristic Curve for Pump B—Suction Lift, 1500 mm.

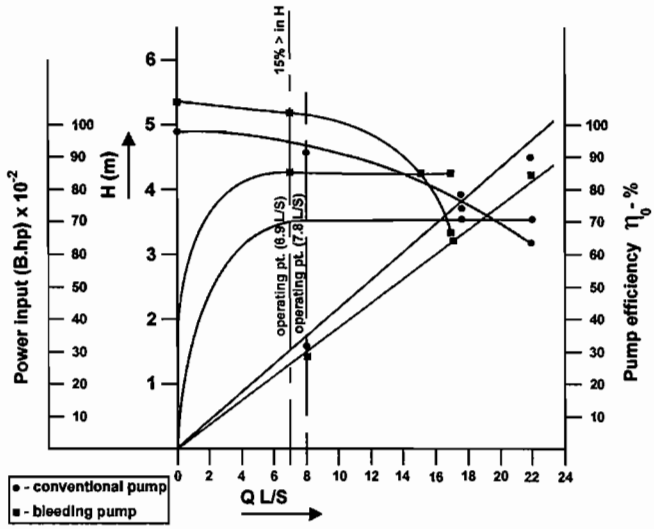

Figure 18. Characteristic Curve for Pump B—Suction Head, 1300 mm.

The relative performance of the three pumps is shown by a nondimensional comparison in Figures 26, 27, and 28, where both the head and the flow are related to the operating (duty) points head (H_0) and flow (Q_0) of the conventional pump for the same preset opening of discharge throttle curve. It can be seen that all the pumps have substantially similar characteristics. Pump B has a larger operating range than the other two pumps.

Figures 11 through 28 suggest that application of a bleeding system using a suitable nozzle arrangement unit placed on the suction side has allowed the control of the pump characteristics from the suction side.

PROTOTYPE

The arrangement for Pump C was chosen to be a prototype for this task. The pump was installed in one of the company's boiler rooms (two boilers, with output of 469 kW, operating pressure ≈ 7 m H_2O, and flow temperature of 80°C). Six pumps of the type similar to Pump C would operate to satisfy the required hot water circulation. The pump was operated continuously at full open bleed for a period of 50 days. Results were consistent for the whole period of its operation. η_0 reached 80 percent as compared to 70 percent without the bleeding system, and the useful lift has risen from 3.1 m to 4.295 m. There was a savings in power input of about 10 percent. Figure 29 shows Pump C with the bleeding system during operation.

CONCLUSIONS

A combined bleeding system using suitable nozzle units and centrifugal pump has been developed with all the characteristics of a centrifugal pump, but at the same time, has a low NPSH capability. NPSH of 70 percent of that of a conventional pump running at the same speed can be attained.

In addition, it was proved that by the use of the new arrangement, higher values of pressure head, higher efficiency, and less energy input are achieved when compared with the performance of a conventional pump.

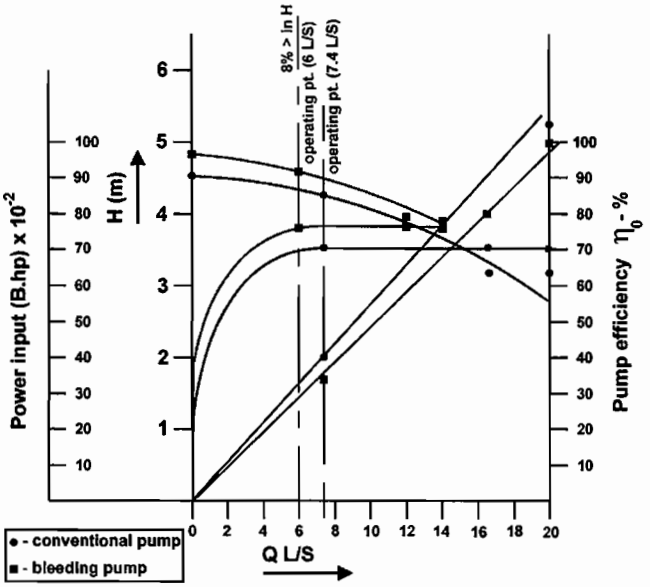

Figure 19. Characteristic Curve for Pump B—Suction Head, 500 mm.

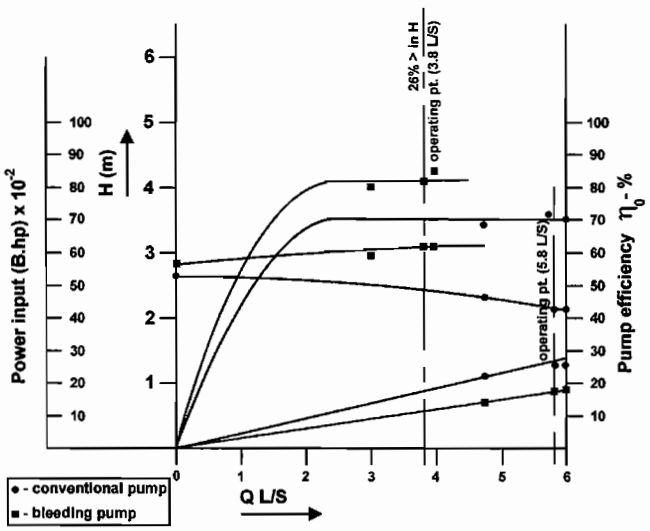

Figure 20. Characteristic Curve for Pump C—Suction Lift, 1300 mm.

Advantages with low NPSH are the ability to reduce holding tank heights (and save construction costs), or to pump fluids that are near their boiling point, or by running the pump faster and replace multistage pumps.

Following the design and development, three pumps were tested to prove the new concept. One of these pumps (Pump C) was chosen as a prototype, to be installed and monitored at-site for a period of three months.

The following themes are to be considered for further research:

• Vortex formation ahead of the impeller in the new system has allowed a greater flow angle at the inlet to that impeller. It is important to note that this new system of bleeding and a better impeller design, having fewer number of vanes than conventional, would lead to a further increase in pump efficiency.

With offshore oil exploration and wells, there is now considerable interest in pumping liquids with a high gas content, as there has been for some time in the pumping systems supplying aircraft gas turbines. The interest is also found within the geothermal practice. The problems are strictly multiphase, but essentially are that as the

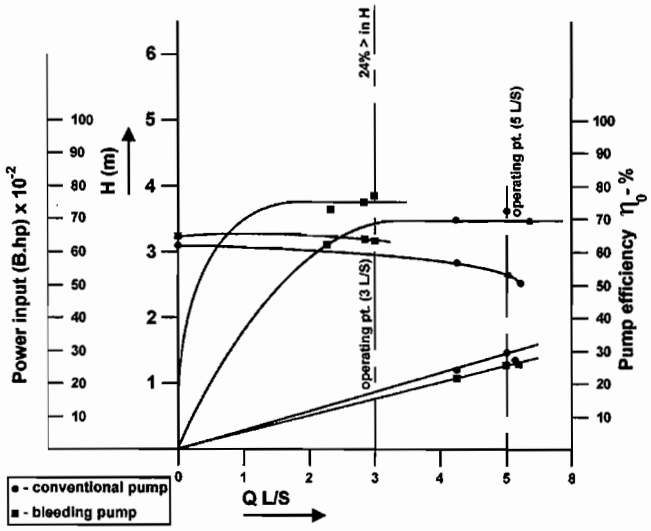

Figure 21. Characteristic Curve for Pump C—Suction Head, 500 mm.

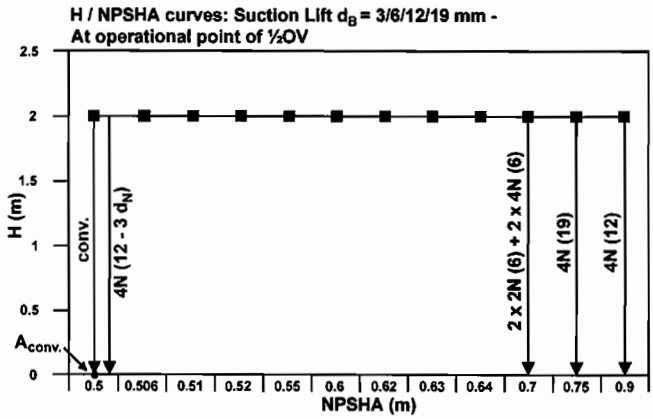

Figure 22. Cavitation Characteristic for Pump A—Suction Lift, 875 mm.

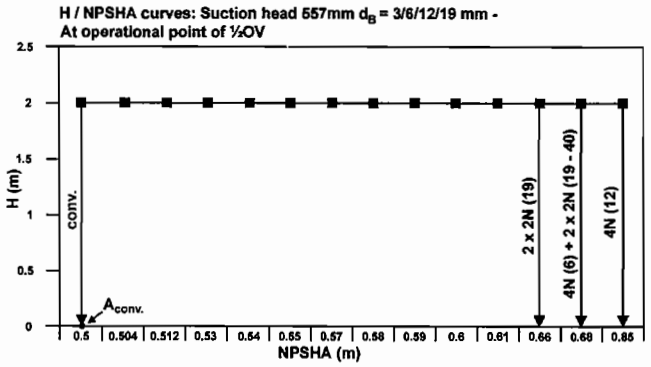

Figure 23. Cavitation Characteristic for Pump A—Suction Head, 556 mm.

gas or steam content increases, the head degrades, when a normal centrifugal pump design is used. Better gas handling is claimed if the blade passages are much larger, and work by Furukawa (1988, 1991) using tandem or slotted blades reduced the degradation in a limited range. Contribution to this problem is also written by Kosmowski (1983), Murakami and Minemura (1974), and Huges and Gordon (1986). With the new arrangement of bleeding, a radical solution is offered as better gas/steam handling is expected when blade passages are made wider by decreasing the number of impeller blades.

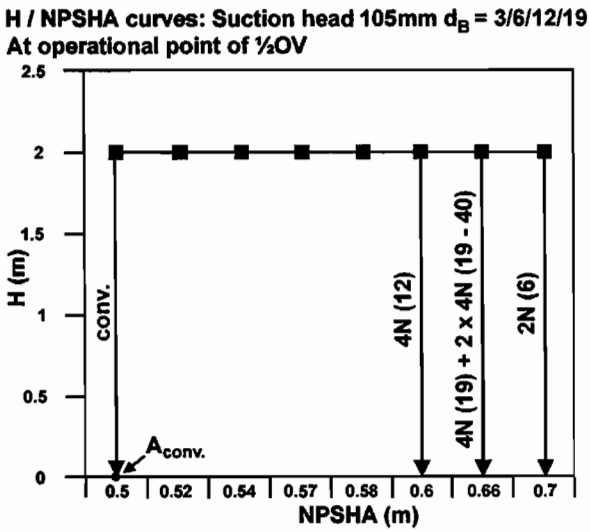

Figure 24. Cavitation Characteristic for Pump A—Suction Head, 105 mm.

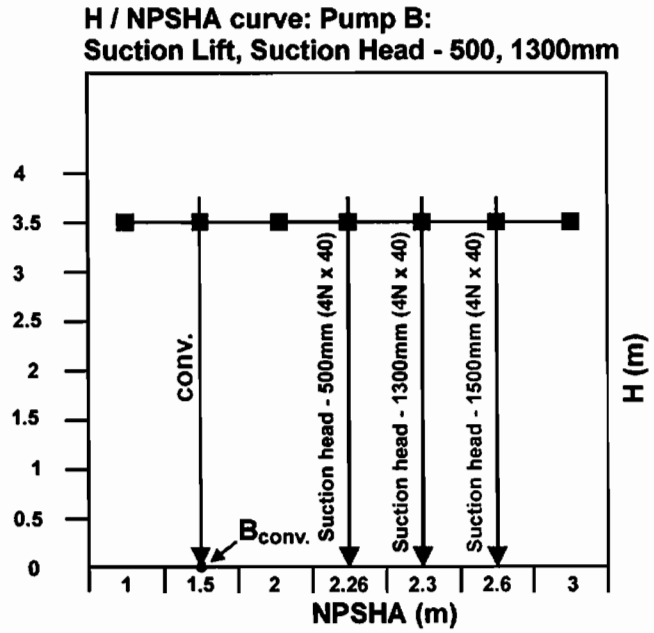

Figure 25. Cavitation Characteristic for Pump B—Suction Lift, 1500 mm; Suction Head, 1300 mm; Suction Head, 500 mm.

- It is the author's opinion that the bleeding concept is also useful when applied to centrifugal fans/blowers.
- Elimination of the spiral volute, and placing a diffuser after the bleeding controls on the discharge line, would reduce losses due to change of energy from pressure to kinetic, thus a further improvement in the performance of the new system is expected.

NOMENCLATURE

A	=	Cross sectional area of nozzle
A_{Conv}	=	Basic point of comparison for $NPSH_A$
B_N	=	Bleeding number = N × A × Cd/Qw
Bhp	=	Brake horsepower = Whp/η_o
b	=	Vane tip length
b_1	=	Vane inlet breadth
b_2	=	Vane exit breadth
C	=	Absolute velocity
C_{1u}	=	Circumferential velocity component on entrance of impeller

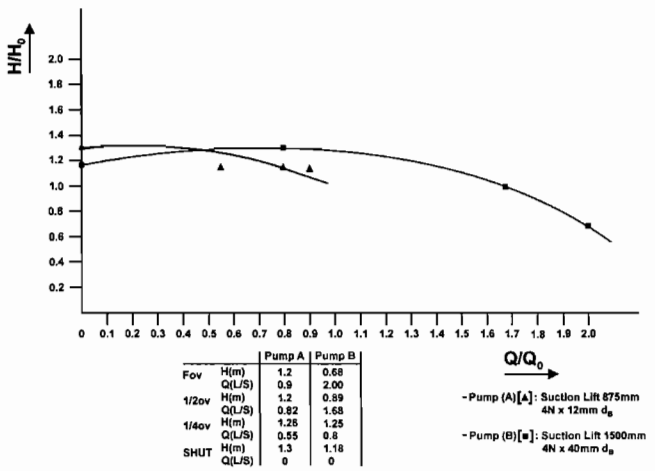

Figure 26. Relative Performance for Pumps A and B. (Pump A—875 mm, Pump B—1500 mm)

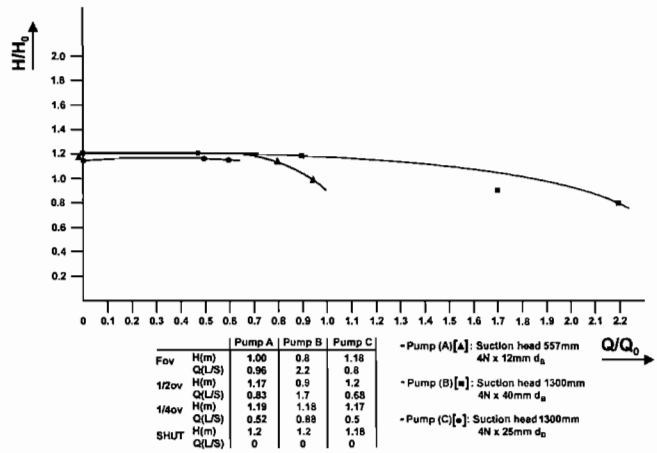

Figure 27. Relative Performance for Pumps A, B, and C. (Pump A—557 mm, Pump B—1300 mm, Pump C—1300 mm)

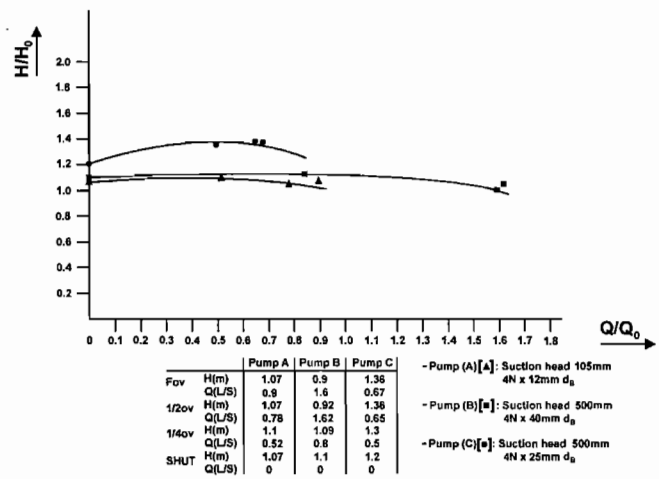

Figure 28. Relative Performance for Pumps A, B, and C. (Pump A—105 mm, Pump B—500 mm, Pump C—500 mm)

C_{2u}	=	Circumferential velocity component on exit
C_a	=	Axial velocity in entrance channel
C_d	=	Fluid velocity at exit from nozzle = Q_d/N × A
d_n	=	Nozzle diameter

Figure 29. Pump C with Bleeding System in Operation—Prototype.

D_d = Delivery pipe internal diameter
D_h = Impeller hub diameter
D_s = Suction pipe internal diameter
d_B = Bleed pipe diameter to nozzle
H_0 = Head at operating point for conventional pump
H = Head at operating point for new arrangement
ΔH = Total head difference between conventional and new pump arrangement at the same discharge
L_n = Nozzle tapered length
M.eff = Mechanical efficiency = 0.98 × Bhp
N = Number of nozzles
n = Speed
N_s = Specific speed (rpm, gpm, ft)
N_{ss} = Suction specific speed (rpm, gpm, ft)
p_1 = Static pressure at entrance of impeller
p_{suc} = Pressure at suction side
Δp = Swelling
Δp_c = Total swelling
Δp_t = Theoretical swelling
Δp_z = Pressure fall in valve
P_{bhp} = Brake horsepower
P_c = Total power
P_b = Power due to secondary losses
P_m = Power loss due to friction in bearings (mechanical)
P_w = Windage power loss
Q_d = Total capacity of stream of fluid through nozzle
Q_0 = Discharge of stream of fluid at operating point (after bleedoff point)
Q_w = Total capacity of a stream of fluid through the impeller
r_1 = Inlet radius to the pump
r_2 = Exit radius to the pump
R_{av} = Average radius between impeller inlet and exit radii
R, r = Radius, radius of curvature at entrance
R_d = Distance from nozzle exit to axis of impeller
Re = Reynolds number
R_{in} = Radius at entrance
R_n = Impeller radius
Ro = Rossby number (Vr/(Rn)—dimensionless group)
R_{ex} = Radius at exit
SG = Specific weight
U_1 = Peripheral velocity at entrance to impeller
U_2 = Peripheral velocity at exit from impeller
V = Absolute velocity of fluid at radius r
w = Relative velocity
Whp = Water horsepower = $Q_w \times SG \times H/550$
β = Entrance angle
η_o = Overall efficiency
λ = Hub/tip ratio = hub diameter to vane length
ν = Kinematic viscosity of liquid
ρ = Density of fluid
φ = Value of nozzle discharge flow coefficient
ω = Angular velocity

APPENDIX A

The mathematical derivation related to design results given under the section, *Bleeding Number*, is stated here for convenience. The basic assumption of the dimensionless group (Bleeding Number) is:

$$B_N = N A C_d / Q_W \tag{A-1}$$

Greater range of control is expected when compared with the effect of rotating action alone.

Theoretically, pressure due to rotation could, in approximation, be calculated for radial pumps as follows:

$$\Delta p_t = \rho g (u_2 C_{2u} - u_1 C_{1u}) \tag{A-2}$$

and for axial pumps:

$$\Delta p_t = \rho g u (C_{2u} - C_{1u}) \tag{A-3}$$

where,

$$u_1 = u_2 = u \tag{A-4}$$

and, the circumferential velocity, C_{1u}, could, in approximation, be calculated from the principle of momentum as follows:

$$\rho Q_d C_d R_d = \rho \int_{R_{in}}^{R_{ex}} 2 \pi R \, dR \, C_a . C_U R \tag{A-5}$$

The distribution of the tangential velocity ahead of a radial impeller can be assumed to follow, in first approximation, the free vortex principle:

$$R_1 C_{U1} = \text{constant} \tag{A-6}$$

Substituting for a radial impeller, we get:

$$Q_d C_d R_d = Q_W R_1 C_{U1} \tag{A-7}$$

C_{1u} is the circumferential velocity that should be checked on an experimental basis.

The above equations do not take into consideration the element of losses. To design a new type of pump we need to know, with the aid of practical measurements, values for the following:

- Circumferential velocity, C_{2u}, using the relation:

$$P_c - P_b - P_m - P_W = \omega M_k = \omega \rho Q_W R_{av} (C_{2u} - C_{1u}) \tag{A-8}$$

where,
P_b = Power lost due to hydraulic loss inside the fluid
P_m = Mechanical power loss
R_{av} = $\frac{1}{2} (R_{in}^2 - R_{ex}^2)$

C_{2u} means the increase in circumferential velocity with radius R.

For a radial impeller we have,

$$R_{av} \approx (R_1 + R_2)/2 \text{ and } Q_W = Q_0 + Q_d \tag{A-9}$$

- C_{1u}: The circumferential (whirl) velocity at the entrance for the impeller is calculated on radius R, which can be determined from the relation:

$$Q_W R_1 C_{1u} = Q_d C_d R_d \tag{A-10}$$

• C_d is the exit velocity from the nozzle, influenced by the value of losses taking place inside the control valves, and can be determined from the relation:

$$C_d = \varphi \left[2\,(\Delta p / \rho)\right]^{1/2} \qquad \text{(A-11)}$$

where,
φ = Nozzle discharge coefficient, selected from test data
$\Delta p = p_{suc} - p_1$

A more accurate relation where the value Δp is decreased by an amount Δp_2 equivalent to loss in pressure inside the control valves and bleed-off line can be used. However a coefficient of flow φ_2 can be derived from actual values in practice. Then we get the relation:

$$C_d = \varphi_2\,(2/\rho\,(\Delta p - \Delta p_2))^{1/2} \qquad \text{(A-12)}$$

The ratio of φ/φ_2 is an indication of the control valve system performance.

• Influence of rotation on centrifugal pumps with a whirl ahead of the impeller can be found by applying the relation:

$$(u_2\,C_{2u} - u_1\;C_{1u})\,\rho g = \Delta p_t \qquad \text{(A-13)}$$

Knowing the value of C_{1u}, the theoretical increase in pressure (rotation) can be easily calculated. With the aid of velocity triangles, losses and useful pressures can be determined.

• The discharge head, H_d, and the suction head, H_s, were measured as follows:

• *Suction head positions*—H_d is measured at the discharge line referred to suction pipe centerline. H_s is measured at the suction line and referred to the same datum.

• *Suction lift positions*—H_d is measured at the discharge line referred to suction pipe centerline. H_s is measured at the suction line, as the distance from the suction liquid level to the same datum.

APPENDIX B

Components of the test facility for Pump A are described.

• *Constant head water tank* (refer to Figure 1)—This is an open tank: 1×0.7×2.2 m^3, elevated 100 mm from ground level. The water in the tank is kept at different reference levels. Delivery from the tank to the suction pipe is through a circular opening 27 mm in diameter. The tank is made of galvanized mild steel, 4 mm sheet thick. A container of 20 liters is positioned near the top side of the tank to measure the volume of discharged water per unit time. In order to diminish the effect of water pulsation inside the tank, two bafflers were installed with a size 132×150×85 mm and 992×200×55 mm, with 550 mm distance apart and 565 mm from the water exit opening.

• *Suction line*—The suction pipe is 297 mm long and made of mild steel. The internal diameter is 27 mm. Arrangement for spacers with different lengths is provided to facilitate positioning of the nozzle units at the desired distance from the impeller. A suction valve is mounted at a distance of 85 mm from the tank edge.

It was important to set the suction pipe as straight and direct as possible, and loops were avoided where air may collect. The new arrangement of the pump is no more sensitive to these factors than the conventional pumps. Nevertheless, if low NPSH performance is required, then every effort should be made to avoid factors that will restrict the NPSH of the plant.

• *Test pump*—The model pump has a centrifugal impeller and a single discharge volute. There is a conical diffuser at the higher-pressure end of the pump. The pump has the following dimensions (Figure B-1):

- r_1 = 10 mm, r_2 = 30 mm, b_1 = 12 mm, b_2 = 8 mm
- Number of vanes = 7 (straight-vane, single-suction)
- H (head) = 2 m (6.56 ft) at Q (discharge) = 0.8 L/s (2.9 m^3/h = 12.7 gpm)
- n (speed) = 1400 rpm, N_s (specific speed) = 1216, N_{ss} (suction specific speed) = 3437
- NPSH = 0.5 m (1.64 ft)

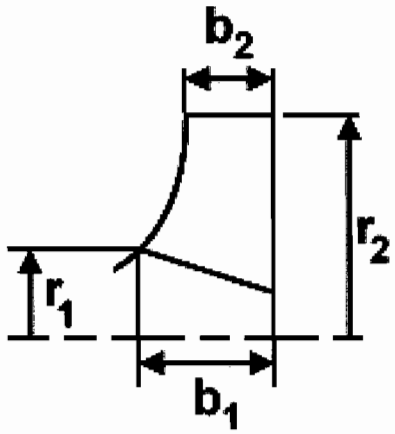

Figure B-1. Pump Dimensions.

• *Electric motor*—The drive motor is asynchronous and runs at the very nearly constant speed of 1400 rpm, with the following characteristics:

- HP = 1/3, Phase = 1, Amperes = 1.1, Hz = 50
- A voltmeter/ampmeter detector is used to measure the voltages and currents consumed, which are recorded during each experiment.

• *Temperature detector*—Mini-surface detectors are used on the external skin of the pipe to measure the fluid (water) temperature, having a measuring range from −50°C up to +250°C. Readings at pump suction and delivery sides were recorded for each experiment.

• *Discharge line*—The discharge pipe is 2.620 m long (for positions 105 and 557 mm), and 4.558 m long (for suction lift position). Pipe is made of PVC, 3 mm thick, and with an internal diameter of 25 mm. The discharge valve is located at a distance of 300 mm from the pump discharge flange. The bleed-off line is positioned before the discharge valve at a distance of 200 mm from the pump discharge flange.

• *Pressure manometer*—Differential pressure measurements are made with the use of a set of two open-tube manometers to read both suction and delivery pressure heads. Readings were registered to be further analyzed. The location of a single pressure tap is 20 mm from impeller inlet, downstream of the nozzle unit. The location of a single discharge pressure tap is 25 mm from discharge flange, downstream of the bleed-off line. The location of suction/discharge pressure is shown in Figure 1.

APPENDIX C

Components of the test facility for Pump B are described (refer to Figure 6).

• *Constant head water tank*—Delivery from tank at suction side is through a circular opening of 100 mm diameter. A container of 150 liters is positioned at the top of the discharge tank. The container dimensions are 750 mm diameter × 960 mm height, made of polyethylene. Two pipes are connecting both suction and discharge tanks. The pipes have the following dimensions:

- Diameters: (1) 96 mm, (2) 150 mm
- Lengths: (1) 1410 mm (2) 1456 mm
- Material: mild steel

• *Suction line*—The suction line is 621 mm long and made of mild steel with an internal diameter of 103 mm and 6 mm thick. A suction valve is mounted at a distance of 225 mm from the tank edge.

• *Test pump*—The model pump is a single-stage mixed flow pump with a single suction. The pump has the following dimensions:

- r_1 = 30 mm, r_2 = 60 mm, b_1 = 90 mm, b_2 = 90 mm
- Number of vanes = 7 (Francis type)
- H (head) = 4.5 m (14.8 ft) at Q (discharge) = 20 L/s (72 m^3/h = 317 gpm)
- n = 1390 rpm, N_s (specific speed) = 3299, N_{ss} (suction specific speed) = 7499
- NPSH = 1.5 m (4.9 ft)

• *Electric motor*—The drive motor runs at a constant speed of 1390 rpm, having the following characteristics:

- HP = 2, Phase = 3, Amperes = 0.2, Hz = 50
- A voltmeter/ampmeter detector reads = 230 V kW = 1.5

• *Temperature detector*—Two mini-surface temperature detectors are used, having a measuring range from −50°C up to +250°C. Readings at suction and delivery sides were recorded for each experiment.

• *Discharge line*—The discharge pipe is 4775 mm long (for positions 500 mm and 1300 mm) and 3895 mm long (for suction lift position). The pipe is made of mild steel, 5 mm thick, and with an internal diameter of 79 mm. The discharge valve is located at a distance of 395 mm from the pump discharge flange.

• *Pressure gauge (piezometer ring)/manometer*—Open-tube manometers were used to measure the pressure head at the suction side. The pressure taps were located 30 mm from the impeller inlet after the nozzle unit.

Gauge manometers were used in measuring the pressure head at the delivery side. One gauge was placed at a distance of 650 mm from the pump discharge flange, at a distance of 255 mm after the throttle discharge valve. The other gauge was located at 40 mm from the pump discharge flange. The gauge was ranged from 0 to 2.5 bars, which was used to measure the discharge pressure.

APPENDIX D

Components of the test facility for Pump C are described.

• *Constant head water tank*—Delivery from tank at the suction side is through a circular opening of 63 mm diameter.

• *Suction line*—The suction pipe is 477 mm long made of mild steel with an internal diameter of 63 mm and 4 mm thick. A suction valve is mounted at a distance of 225 mm from the tank edge.

• *Test pump*—The model pump is a single-stage centrifugal glanded pump with a single-suction impeller, having the following dimensions:

- r_1 = 30 mm, r_2 = 60 mm, b_1 = 10 mm, b_2 = 8 mm
- Number of vanes = 7 (straight-vane, single-suction, closed impeller)
- H (head) = 3.5 m (11.5 ft) at Q (discharge) = 5 L/s (18 m^3/h = 79.3 gpm)
- n (speed) = 1450 rpm N_s (specific speed) = 2066 N_{ss} (suction specific speed) = 6588
- NPSH = O.75 m (2.5 ft)

• *Electric motor*—The drive motor runs at a constant speed of 1450 rpm, having the following characteristics:

- HP = 0.4, Phase =3, Amperes = 3.5, Hz = 50
- A voltmeter/ampmeter detector reads = 405 V kW = 0.3

• *Discharge line*—The discharge pipe is 4385 mm long (for positions 500 mm and 1300 mm). The pipe is made of mild steel, 4 mm thick, and with an internal diameter of 63 mm. The discharge valve is located at a distance of 290 mm from the pump discharge flange.

• *Pressure gauge (piezometer ring)/manometer*—Open-tube manometers were used to measure the pressure head at the suction side. The pressure tap was located 20 mm from inlet to impeller after the nozzle unit.

Gauge manometers were used in measuring the pressure head at the delivery side. One gauge was placed at a distance of 440 mm from the pump discharge flange, at a distance of 150 mm after the throttle discharge valve. The other gauge was located 30 mm from the pump discharge flange, which was used to measure the pump head.

APPENDIX E

Performance Characteristics

This section lists the results for the total range of nozzle units used for Pump A, B, and C, at different levels.

• Pump A—Suction lift (875 mm)

Table E-1. Performance Characteristics for Pump A—Suction Lift, 875 mm.

		2N-12mm		4N-12mm		2x2N-12mm		2x4N-12mm 80 apart		2x4N-12mm 40 apart		4N-12(3dn)	
		conv.	Bleed	conv.	Bleed	conv.	Bleed	conv.	Bleed	conv.	Bleed	conv.	Bleed
	W.hp.	0.225	0.2	0.21	0.2	0.22	0.19	0.22	0.14	0.22	0.14	0.23	0.17
	M.eff.	0.7	0.685	0.7	0.68	0.7	0.68	0.7	0.675	0.7	0.675	0.7	0.68
	B.hp.	0.32	0.25	0.29	0.25	0.31	0.24	0.32	0.175	0.3	0.15	0.33	0.22
FOV	H(m)	1.99	2.1	1.89	2.3	1.99	2.1	1.96	2.1	1.96	2.1	1.96	2
	Q(L/S)	0.85	0.77	0.83	0.66	0.83	0.67	0.85	0.47	0.83	0.5	0.87	0.66
½OV	H(m)	2	2.1	1.9	2.3	2	2.12	2	2.1	2	2.13	2.1	2.1
	Q(L/S)	0.72	0.67	0.73	0.6	0.71	0.58	0.71	0.4	0.7	0.45	0.67	0.5
¼OV	H(m)	2.1	2.2	2	2.4	2.1	2.2	2.1	2.2	2.1	2.17	2.1	2.15
	Q(L/S)	0.46	0.44	0.47	0.4	0.45	0.4	0.43	0.27	0.44	0.3	0.37	0.33
SHUT	H(m)	2.25	2.24	2.1	2.55	2.2	2.2	2.2	2.2	2.2	2.2	2.15	2.15
	Q(L/S)	0	0	0	0	0	0	0	0	0	0	0	0
FOV	$\eta_{overall}$	0.7	0.8	0.7	0.8	0.7	0.78	0.7	0.8	0.73	0.93	0.69	0.77
½OV	$\eta_{overall}$	0.7	0.78	0.7	0.78	0.7	0.82	0.7	0.86	0.71	0.8	0.68	0.8
¼OV	$\eta_{overall}$	0.7	0.86	0.7	0.83	0.7	0.78	0.7	0.79	0.7	0.8	0.68	0.77

B.hp - Q : 4N-12mm (Suction Lift : 875mm)

	Full Open		½ Open		¼ Open		SHUT	
	conv.	Bleed	conv.	Bleed	conv.	Bleed	conv.	Bleed
B.hp.	0.0298	0.025	0.0264	0.023	0.0178	0.015	0	0
Q(L/S)	0.83		0.73		0.47		0	

• Pump A—Suction head (557 mm)

Table E-2. Performance Characteristics for Pump A—Suction Head, 557 mm.

		2N-12mm		4N-12mm		2x2N-12mm 40		2x4N-19mm 80		2x4N-19mm 40	
		conv.	Bleed	conv.	Bleed	conv.	Bleed	conv.	Bleed	conv.	Bleed
	W.hp.	0.236	0.2	0.226	0.19	0.22	0.19	0.25	0.16	0.24	0.16
	M.eff.	0.7	0.685	0.7	0.68	0.7	0.68	0.7	0.675	0.7	0.675
	B.hp.	0.337	0.25	0.32	0.23	0.32	0.25	0.36	0.21	0.33	0.23
FOV	H(m)	1.77	1.8	1.7	2	1.7	1.9	1.9	2	1.77	1.89
	Q(L/S)	1	0.87	1	0.8	0.99	0.77	1	0.6	1	0.66
½OV	H(m)	1.8	1.85	1.7	2.05	1.8	1.9	1.9	2	1.8	1.88
	Q(L/S)	0.8	0.74	0.83	0.69	0.83	0.6	0.83	0.5	0.83	0.55
¼OV	H(m)	1.88	1.87	1.8	2.08	1.87	1.9	2	2	1.88	1.9
	Q(L/S)	0.5	0.47	0.48	0.43	0.48	0.4	0.5	0.33	0.48	0.36
SHUT	H(m)	1.89	1.9	1.8	2.1	1.79	1.9	2	2	1.89	1.93
	Q(L/S)	0	0	0	0	0	0	0	0	0	0
FOV	$\eta_{overall}$	0.7	0.8	0.69	0.83	0.7	0.78	0.69	0.76	0.7	0.72
½OV	$\eta_{overall}$	0.7	0.76	0.69	0.84	0.7	0.072	0.7	0.74	0.7	0.72
¼OV	$\eta_{overall}$	0.69	0.68	0.7	0.79	0.7	0.76	0.7	0.7	0.69	0.7

B.hp - Q : 4N-12mm (Suction head : 557mm)

	Full Open		½ Open		¼ Open		SHUT	
	conv.	Bleed	conv.	Bleed	conv.	Bleed	conv.	Bleed
B.hp.	0.0324	0.0255	0.0323	0.025	0.0164	0.015	0	0
Q(L/S)	1.00		8.0		0.48		0	

- Pump A—Suction head (105 mm)

Table E-3. Performance Characteristics for Pump A—Suction Head, 105 mm.

		2N-12mm		4N-12mm		2x2N-12mm		2x4N-12mm 80		2x4N-12mm 40	
		conv.	Bleed	conv.	Bleed	conv.	Bleed	conv.	Bleed	conv.	Bleed
	W.hp.	0.24	0.219	0.24	0.2	0.24	0.19	0.24	0.14	0.25	0.15
	M.eff.	0.7	0.685	0.7	0.68	0.7	0.68	0.7	0.675	0.7	0.675
	B.hp.	0.34	0.3	0.34	0.24	0.34	0.24	0.35	0.2	0.36	0.19
FOV	H(m)	2	2.06	2	2.15	2	2.1	2	2.13	2.1	2.2
	Q(L/S)	0.9	0.8	0.9	0.7	0.9	0.68	0.91	0.5	0.91	0.5
½OV	H(m)	2	2.1	2	2.15	2	2.1	2	2.14	2.15	2.22
	Q(L/S)	0.5	0.7	0.77	0.6	0.76	0.58	0.77	0.4	0.78	0.44
¼OV	H(m)	2.1	2.2	2.1	2.2	2.1	2.2	2.1	2.15	2.16	2.19
	Q(L/S)	0.44	0.42	0.44	0.4	0.44	0.37	0.45	0.29	0.44	0.3
SHUT	H(m)	2.1	2.2	2	2.15	2.1	2.2	2	2.2	2.2	2.27
	Q(L/S)	0	0	0	0	0	0	0	0	0	0
FOV	$\eta_{overall}$	0.69	0.73	0.69	0.79	0.69	0.79	0.69	0.71	0.7	0.77
½OV	$\eta_{overall}$	0.7	0.73	0.7	0.8	0.7	0.77	0.7	0.76	0.7	0.76
¼OV	$\eta_{overall}$	0.7	0.77	0.7	0.72	0.7	0.775	0.7	0.75	0.7	0.73

B.hp - Q : 4N-12mm (Suction head : 105mm)

	Full Open		½ Open		¼ Open		SHUT	
	conv.	Bleed	conv.	Bleed	conv.	Bleed	conv.	Bleed
B.hp.	0.0373	0.024	0.029	0.021	0.0176	0.016	0	0
Q(L/S)	0.9		0.77		0.44		0	

- Pump B

Table E-4. Performance Characteristics for Pump B.

		4N-40mm (A) Suction Lift 1500mm		4N-40mm (B) Suction head 1300mm		4N-40mm (B) Suction head 500mm	
		conv.	Bleed	conv.	Bleed	conv.	Bleed
	W.hp.	0.65	0.56	0.64	0.56	0.68	0.52
	M.eff.	0.7	0.85	0.7	0.85	0.7	0.75
	B.hp.	0.94	0.65	0.91	0.65	0.97	0.69
FOV	H(m)	2.63	3	3.15	3.57	3.14	3.85
	Q(L/S)	19	14	22	17	20	14
½OV	H(m)	3.13	3.94	3.6	3.98	3.19	3.95
	Q(L/S)	15	11.8	17	13	16.5	12
¼OV	H(m)	4.4	5.5	4.4	5.2	4.27	4.66
	Q(L/S)	7	5.7	7.8	6.9	7.4	6
SHUT	H(m)	4.75	5.19	4.9	5.3	0.45	4.83
	Q(L/S)	0	0	0	0	0	0
FOV	$\eta_{overall}$	0.7	0.86	0.7	0.86	0.7	0.75
½OV	$\eta_{overall}$	0.69	0.85	0.69	0.85	0.7	0.758
¼OV	$\eta_{overall}$	0.68	0.86	0.68	0.86	0.7	0.76

B.hp - Q : 4N-40mm (Suction Lift : 1500mm)

	Full Open		½ Open		¼ Open		SHUT	
	conv.	Bleed	conv.	Bleed	conv.	Bleed	conv.	Bleed
B.hp.	1.08	0.87	0.87	0.71	0.38	0.32	0	0
Q(L/S)	19		15		7		0	

B.hp - Q : 4N-400mm (Suction head : 1300mm)

	Full Open		½ Open		¼ Open		SHUT	
	conv.	Bleed	conv.	Bleed	conv.	Bleed	conv.	Bleed
B.hp.	0.9	0.85	0.75	0.65	0.3	0.27	0	0
Q(L/S)	22		17		7.8		0	

B.hp - Q : 4N-400mm (Suction head : 500mm)

	Full Open		½ Open		¼ Open		SHUT	
	conv.	Bleed	conv.	Bleed	conv.	Bleed	conv.	Bleed
B.hp.	1.11	1	0.94	0.8	0.4	0.34	0	0
Q(L/S)	20		16.5		7.4		0	

- Pump C

Table E-5. Performance Characteristics for Pump C.

		4N-25mm (A) Suction head 500mm		4N-25mm (B) Suction head 1300mm	
		conv.	Bleed	conv.	Bleed
	W.hp.	0.18	0.128	0.18	0.16
	M.eff.	0.7	0.75	0.7	0.8
	B.hp.	0.28	0.15	0.26	0.18
FOV	H(m)	2.7	3.2	2.26	3.1
	Q(L/S)	5	3	6	3.9
½OV	H(m)	2.47	3.23	2.27	3.1
	Q(L/S)	5.2	2.9	5.8	3.8
¼OV	H(m)	2.85	3.17	2.48	3
	Q(L/S)	4.2	2.5	4.7	3
SHUT	H(m)	3.1	3.2	2.69	2.8
	Q(L/S)	0	0	0	0
FOV	$\eta_{overall}$	0.69	0.77	0.7	0.84
½OV	$\eta_{overall}$	0.71	0.75	0.72	0.82
¼OV	$\eta_{overall}$	0.69	0.73	0.69	0.8

B.hp - Q : 4N-25mm (Suction head : 500mm)

	Full Open		½ Open		¼ Open		SHUT	
	conv.	Bleed	conv.	Bleed	conv.	Bleed	conv.	Bleed
B.hp.	0.28	0.25	0.26	0.25	0.23	0.2	0	0
Q(L/S)	5.00		5.2		4.2		0	

B.hp - Q : 4N-25mm (Suction head : 1300mm)

	Full Open		½ Open		¼ Open		SHUT	
	conv.	Bleed	conv.	Bleed	conv.	Bleed	conv.	Bleed
B.hp.	0.26	0.24	0.25	0.23	0.23	0.2	0	0
Q(L/S)	6.00		5.8		4.7		0	

REFERENCES

Duncan, A. B., McColl J. R., and Bocking A., 1971, "Recent Trends in Development of Large Process Pumps," Conference on Process Pumps, Durham, United Kingdom.

Furukawa, A., 1988, "Fundamental Studies on a Tandem Blades Impeller of Gas Liquid Two-Phase Centrifugal Pump," Memoirs of the Faculty of Engineering Kyushu University, *48*, (4), pp. 231-240.

Furukawa, A., 1991, "On an Improvement in Air/Water Two Phase Flow Performance of a Centrifugal Pump in the Partial Flow Rate Range of Water," Sixty-Ninth JSME Fall Annual Meeting, *B*, Paper Number 1118, pp. 165-167.

Huges, S. J. and Gorden, I., July 1986, "Multi-Phase Research for North Sea Oil and Gas Production," J. Mar. Rev., pp. 4-9.

Kosmoswski, I., 1983, "The Design of Centrifugal Pumps for a Delivery of Liquids with High Gas Content," Eighth BPMA Tech. Conf., Paper 13.

Kratzer, A., 1975, "Corrosion and Erosion Damage to Chemical Centrifugal Pumps," Fourth Conference of British Pump Manufacturers Association, Durham, United Kingdom.

Murakami, M. and Minemura, K., 1974, "Effects of Entrained Air on the Performance and Flow Conditions," Bulletin of JSME, *17*, (110), p. 1047.

Pearsall, I. S. and Sobie, G, July 1970, "Pumps for Low Suction Pressures" *Chemical and Process Engineering*, p. 83.

Reddy, Y. R. and Pickford, J. A., 1979, "Swirl Angle Distribution in Pump Inlets in Circular Sump," Sixth Conference of British Pump Manufacturers Association, University of Kent, Canterbury, England.

Sutton, M., 1967, "The Inducer: A Means of Improving the Suction Performance of Centrifugal Pumps," British Hydro-Mechanics Research Association, REP. No. RR889.

BIBLIOGRAPHY

Anderson, H. H., 1974, "Modern Development in the Use of Large Single Entry Centrifugal Pumps," Conference on Cavitation, Edinburgh, England.

ACKNOWLEDGEMENT

This work was funded by Unitec Institute of Technology via a cooperative research agreement with the author. The author is grateful to Jack Verbiesen, Rhys Davey, and Godfrey Gomes for the provision of test rigs and for their assistance during the tests. Dr. Martin Hall, Dean for the Faculty of Applied Skills, is thanked for offering great encouragements and continuous support during the different stages of the project.